

Noisy monitored quantum dynamics of ergodic multi-qubit systems

Henning Schomerus

Department of Physics, Lancaster University, Lancaster, LA1 4YB, United Kingdom

I employ random-matrix methods to set up and solve statistical models of noisy nonunitary dynamics that appear in the context of monitored quantum systems. The models cover a range of scenarios combining random dynamics and measurements of variable strength of one or several qubits. The combined dynamics drive the system into states whose statistics reflect the competition of randomizing unitary evolution and the measurement-induced backaction collapsing the state. These effects are mediated by entanglement, as I describe in detail by analytical results. For the paradigmatic case of monitoring via a single designated qubit, this reveals a simple statistical mechanism, in which the monitoring conditions the state of the monitored qubit, which then imposes statistical constraints on the remaining quantities of the system. For the case of monitoring several qubits with prescribed strength, the developed formalism allows one to set up the statistical description and solve it numerically. Finally, I also compare the analytical results to the monitored dynamics of a quantum kicked top, revealing two regimes where the statistical model either describes the full stationary dynamics, or resolves time scales during particular parts of the evolution.

The conceptual understanding of the role of measurements in quantum mechanics has significantly evolved over time [1–3]. Being rooted in a probabilistic description, a notable aspect of this discussion has been how the theory should be interpreted when applied to individual quantum systems, as well as individual parts of composed systems. As for the understanding of measurements carried out on a subsystem, entanglement has been identified as a key signature that sets quantum systems apart from classical ones. In turn, the developments around experimental demonstrations of entanglement have shed significant light on the interpretation of the theory in individual realizations. A central feature of entanglement is that it is only useful if the state of the system is known to a sufficient extent. For instance, a random incoherent mixture of fully entangled states is completely indistinguishable from a mixture of separable states. But with advances in quantum optics and the recent advent of noisy intermediate scale quantum devices, quantum systems can be monitored and controlled in detail, justifying an approximate description by pure states even through the monitoring phase. Nonetheless, such monitoring leaves a significant impact on the dynamics, the backaction, whose early manifestation was the collapse of the wave function. This backaction differs from the quantum dynamics of the isolated system in that it is non-unitary, which results from the conditioning of the quantum state according to the measurement outcome. The backaction is just as central to the description of measurements, as it means that monitoring is indeed useful—it entails that the measurement outcomes indeed reveal information about the quantum state, to the extent that in a complete measurement the outcomes pinpoint a definite, pure, post-measurement state. However, this requires to have access to all outcomes, as otherwise the measurement has the opposite effect of turning a pure state into an effectively mixed state.

These considerations enjoy a significant generalization when one considers the interaction of a quantum system with its environment—as pioneered, amongst others, by

Fritz Haake, who developed comprehensive statistical descriptions of open quantum systems [4], and applied these both to specific paradigms as well as to advance the conceptual interpretation of the measurement process (for a brief overview of this oeuvre see [5]). This laid the ground for our present understanding, in which many of the key aspects of measurements and open-system dynamics can be captured in a unified language. In this, entanglement with the environment gives rise to decoherence, which manifests itself in a reduced purity of the density matrix, meaning that the system effectively evolves into a mixed state. In turn, recording these interactions in sufficient detail can reveal enough information to protect the pure-state dynamics, as is manifested in weak, continuous, or variable strength measurements.

These conceptual advances also have guided the development of powerful theoretical approaches. As a statistical tool, pure-state dynamics is useful as it can be averaged over incoherently to capture the general case of mixed-state dynamics, leading to frameworks such as quantum jump and trajectory formulations of unravelled master equations [6]. And over the recent years, considering the pure-state dynamics in complex quantum circuits has brought about significant insights into the interplay of dynamical entanglement generation and spreading and the reduction of entanglement in local measurements [7–29]. This revealed a measurement-induced phase transition in the entanglement entropy, which changes from an extensive to an intensive quantity (a volume law to an area law) when the measurement strength exceeds a certain value. While initially encountered in a stroboscopic setting with maximally random local dynamics and hard measurements, this transition is now known to occur in a wide range of related settings, and in particular, also for continuously evolving systems monitored with variable strength [30, 31].

It is against the backdrop of these systems that I formulate, in this paper, a statistical description of noisy monitored pure-state dynamics in multi-qubit systems. In contrast to the works concerning the entanglement

transition, I here consider noisy dynamics in which all qubits interact on equal terms. Furthermore, instead of monitoring all of the qubits, I focus on the case that this is done for a specific designated subset of the qubits, which are subjected to variable-strength measurements. In absence of the monitoring, the dynamics displays universal behaviour in accordance to random-matrix theory, another field of significant activity in Fritzens work [32]. This sets a benchmark to investigate how monitoring the qubits affects the quantum state of the complete system, revealing the role of correlations and entanglement in mediating the backaction to other parts of the system. I also take the opportunity to apply these results to a specific physical setting, the monitored dynamics of a kicked quantum top [33], the paradigmatic model that Fritz introduced to study how complex systems display the quantum signatures of chaos [32].

The underlying physics is most clearly revealed in noisy systems that are monitored with variable strength via a single designated qubit. In this case, we can obtain comprehensive analytical results for the statistical features of the quantum state in the stationary limit of long times. In this statistical description, it turns out that all nontrivial effects of the monitoring on the dynamics can then be captured by a single quantity, and the geometric constraints that this quantity poses on others. This quantity, which we will denote as r , simply represents the probability that the monitored qubit is in the state $|0\rangle$ in the monitoring basis. The underlying physical picture is that besides the monitoring-induced conditioning on r , the quantum state of the composed system is statistically free. The intriguing feature is how powerful these r -dependent constraints are in transferring the effects of the monitoring to other parts of the system. This results in highly complex and characteristic statistical signatures of the monitoring as a function of its strength, which we reveal by adopting parameterizations that highlight the role of correlations and entanglement. These features also extend to the case of monitoring several of the qubits with possibly distinct strength, where results can be obtained by numerical solution of the statistical model. Finally, the comparison of the analytical results of the monitored noisy dynamics to the monitored dynamics of the quantum kicked top [33] reveals two regimes, where the statistical model either describes the full stationary dynamics in the kicked top, or resolves the deterministic dynamical time scales during particular parts of its evolution.

This work is organised as follows. Section I describes the general setting and the properties of the quantum state we are interested in, and sets out the monitoring protocol. Section II addresses the noisy dynamics in the absence of monitoring, which serves as a benchmark for the monitored dynamics, and allows us to develop the general methodology, which is closely related to Dyson's Brownian motion approach [34]. With Section III, we turn to the instructive case of multi-qubit systems monitored by a single designated qubit, for which we can ob-

tain exact analytical results. Section IV complements this with numerical results for systems with multiple monitored qubits. In Sec. V, I then compare the analytical results of Sec. III to the monitored dynamics of a kicked top. The results are summarised in the concluding Sec. VI, which also describes further implications and gives an outlook on possible extensions.

I. SETTING

We are interested in the dynamics of quantum systems under repeated steps of random unitary evolution and variable-strength measurements. This section describes the types of systems along with their quantities of interest, as well as the applied measurement protocol. In the next sections this is then applied to various dynamical scenarios.

A. Systems and quantities of interest

We consider the pure-state dynamics $|\psi(t)\rangle$ of quantum systems with a finite Hilbert-space dimension N , which will come about by the combination of unitary time evolution and measurement steps with recorded outcomes. We denote the amplitudes in the natural computational basis $|n\rangle$ as $\psi_n = \langle n|\psi\rangle$, and will be particularly interested in the statistics of the normalised probability coefficients

$$r_n = |\psi_n|^2, \quad \sum_n r_n = 1 \quad (1)$$

attained at large times.

Our main focus will be on systems made out of one or several two-level systems (here referred to as qubits), where the Hilbert space is a tensor product of q two-dimensional spaces, and overall $N = 2^q$, where we let indices run from $n = 1$ to N . For a single-qubit system, we write explicitly

$$|\psi\rangle = \alpha|0\rangle + \beta|1\rangle \quad (2)$$

and set

$$r = |\alpha|^2 = 1 - |\beta|^2. \quad (3)$$

For a two-qubit system, we write

$$|\psi\rangle = \alpha|00\rangle + \beta|01\rangle + \gamma|10\rangle + \delta|11\rangle \quad (4)$$

and set

$$r = |\alpha|^2 + |\beta|^2 = 1 - |\gamma|^2 - |\delta|^2, \quad (5)$$

$$R = |\alpha|^2 + |\gamma|^2 = 1 - |\beta|^2 - |\delta|^2, \quad (6)$$

$$C = |\alpha|^2|\delta|^2 - |\beta|^2|\gamma|^2. \quad (7)$$

Here r and R are the probabilities to find the first or second qubit in the state $|0\rangle$. The quantity C quantifies the

experimentally observable correlations of the measurement outcomes specifically carried out in the computational basis, and will feature naturally in the statistical analysis. For this, we will make use of the following relations,

$$|\alpha|^2 = C + rR, \quad |\beta|^2 = r(1 - R) - C, \quad (8)$$

$$|\gamma|^2 = R(1 - r) - C, \quad |\delta|^2 = (1 - r)(1 - R) + C. \quad (9)$$

Furthermore, we will also consider the concurrence

$$C = 2|\alpha\delta - \beta\gamma|, \quad (10)$$

which quantifies the degree of entanglement as detectable by combining measurements inside and outside the computational basis.

For a system of q qubits, we work with the probability coefficients r_n defined in Eq. (1), as well as with the probability coefficients

$$R_m = \sum_{n|\text{qubit } m \text{ in state } |0\rangle} r_n \quad (11)$$

of the individual qubits, and where convenient abbreviate

$$\begin{aligned} r &\equiv R_1 = \sum_{n=1}^{N/2} r_n, \\ R &\equiv R_2 = \sum_{n=1}^{N/2} r_{2n-1}, \end{aligned} \quad (12)$$

for the probability to find the first or second qubit in state $|0\rangle$.

B. Measurement protocol

We implement measurements of variable strength λ by controlled entanglement with a suitable auxiliary system, whose state is then measured and the outcome recorded. The measurements are assumed to occur instantaneously, where pre-measurement states are denoted by a time index t_- and post-measurement states by a time index t_+ . Depending on the measurement protocol, this can be designed to either extract information discriminating all states of the system, or only those of a subsystem. We here set this out for the case of one and two qubits, and refer to Appendix A for a general version of this protocol for a system of N states.

1. Description for a single qubit

Denoting the normalised state of a single qubit as

$$|\psi(t_-)\rangle = \alpha|0\rangle + \beta|1\rangle, \quad (13)$$

we first entangle it with an ancilla qubit. This is designed to take the initially separable joint state

$$|\varphi\rangle = |\psi(t_-)\rangle \otimes |0\rangle \quad (14)$$

into the intermediate state

$$|\varphi\rangle = \alpha|0\rangle \otimes |a_\lambda\rangle + \beta|1\rangle \otimes |a_{-\lambda}\rangle, \quad (15)$$

$$|a_\lambda\rangle = \sqrt{\frac{1+\lambda}{2}}|0\rangle + \sqrt{\frac{1-\lambda}{2}}|1\rangle, \quad (16)$$

where $\lambda \in [0, 1]$ determines the measurement strength. In a quantum circuit, this step can be implemented by a conditional gate operation. Measuring the ancilla in its computational basis brings the system back into a separable state, which depends on the measurement outcome. We use an index $\eta = \pm 1$ to distinguish the two possibilities, $\eta = 1$ if the ancilla is found in state $|0\rangle$ and $\eta = -1$ if the ancilla is found in state $|1\rangle$. Post-measurement, the qubit of interest then assumes the state

$$|\psi_\eta(t_+)\rangle = \frac{\sqrt{1+\eta\lambda}\alpha|0\rangle + \sqrt{1-\eta\lambda}\beta|1\rangle}{\sqrt{1+\eta\lambda(|\alpha|^2 - |\beta|^2)}}. \quad (17)$$

These outcomes occur with probabilities

$$P_\eta = \frac{1 + \lambda\eta(|\alpha|^2 - |\beta|^2)}{2}. \quad (18)$$

The effect that the quantum state changes upon the measurement is generally known as backaction. According to (17), this here modifies the probability coefficient to

$$r_{t_+} = \frac{(1 + \eta\lambda)r_{t_-}}{1 + \eta\lambda(2r_{t_-} - 1)}. \quad (19)$$

Averaged over the measurement outcomes $\eta = \pm 1$, we then always have

$$\overline{r_{t_+}} = r_{t_-}. \quad (20)$$

For measurement strength $\lambda = 1$, this description reduces to the standard von Neumann protocol of projective measurements, while general values $0 < \lambda < 1$ result in variable-strength measurements. If λ is small, we can approximate the backaction by the following simplified description,

$$r_{t_+} = r_{t_-} + dr_{t_-}, \quad (21)$$

$$dr \equiv 2\xi\lambda r(1 - r), \quad (22)$$

where $\xi = \pm 1$ again signals random measurement outcomes, but these are now taken to occur with equal, state-independent probability $P(\xi = \pm 1) = 1/2$. As indicated in our notation, we defined the increments so that they refer to the initial data (Ito calculus), and in a way where we can then drop the time index. The increment dr correctly reproduces the first and second moment of the backaction on the coefficient in the leading orders of the measurement strength,

$$\overline{dr} = 0 + O(\lambda^3), \quad (23)$$

$$\overline{(dr)^2} = 4\lambda^2 r^2(1 - r^2) + O(\lambda^3). \quad (24)$$

When interpreted stochastically, these equations can be used to describe the continuous monitoring of the system, which is the regime that we will focus on in this paper. In this case, the measurement backaction effectively scales as λ^2 , which we later quantify relative to a similar scaling of noisy unitary dynamics in the considered systems.

2. Description for two qubits

The protocol for a single qubit can be extended to multiple qubits in several ways. Here, we describe the situation that we monitor one of the qubits. Because observables of distinct qubits commute, the case where both qubits are monitored then simply follows from composition of these measurements. The closely related case to monitor the composed system with an auxiliary 4-level system is covered by the general protocol for N -level systems, described in Appendix A.

We designate the first qubit as the monitored one, which is again achieved by utilizing an ancilla. The physical entanglement and measurements steps are the same as for the isolated qubit, resulting in the post-measurement state

$$|\psi_\eta(t_+)\rangle = \frac{\sqrt{1+\eta\lambda}}{\sqrt{2P_\eta}}(\alpha|00\rangle+\beta|01\rangle) + \frac{\sqrt{1-\eta\lambda}}{\sqrt{2P_{-\eta}}}(\gamma|10\rangle+\delta|11\rangle), \quad (25)$$

where the outcomes $\eta = \pm 1$ now occur with probability

$$P_\eta = \frac{1 + \lambda\eta(|\alpha|^2 + |\beta|^2 - |\gamma|^2 - |\delta|^2)}{2}. \quad (26)$$

In terms of the parameterization (9), this gives

$$r_{t_+} = \frac{(1 + \eta\lambda)r_{t_-}}{1 + \eta\lambda(2r_{t_-} - 1)}, \quad (27)$$

$$R_{t_+} = R_{t_-} + \frac{2C_{t_-}\eta\lambda}{1 + \eta\lambda(2r_{t_-} - 1)}, \quad (28)$$

$$C_{t_+} = C_{t_-} \frac{1 - \lambda^2}{(1 + \eta\lambda(2r_{t_-} - 1))^2}. \quad (29)$$

We see that the backaction also affects the probability coefficient R of the other qubit, and that this is mediated via the correlation parameter C .

For small measurement strength λ , we can again obtain the backaction from a simplified stochastic process, with increments

$$dr = 2\xi\lambda r(1-r), \quad (30)$$

$$dR = 2\xi\lambda C, \quad (31)$$

$$dC = 2\lambda C((1-2r)\xi - 2\lambda r(1-r)) \quad (32)$$

and $\xi = \pm 1$ again occurring with equal, state-independent probability $P(\xi = \pm 1) = 1/2$.

An analogous process is obtained when we monitor the second qubit with strength λ' and monitoring noise ξ' ,

and both can be combined into a single process given by

$$dr = 2\xi\lambda r(1-r) + 2\xi'\lambda' C, \quad (33)$$

$$dR = 2\xi'\lambda' R(1-R) + 2\xi\lambda C, \quad (34)$$

$$dC = 2C[\xi\lambda(1-2r) - 2\lambda^2 r(1-r) + \xi'\lambda'(1-2R) - 2\lambda'^2 R(1-R)]. \quad (35)$$

This composition is valid because the noise variables ξ and ξ' are independent of each other, and analogous considerations will allow us to extend these descriptions further to include noisy unitary dynamics.

C. The role of monitoring

If we do not have access to the outcomes, the measurements induce decoherence and drive the system into a mixed state, with the decoherence rate governed by λ (in the continuous case, scaling as λ^2). In the context of monitored dynamics, however, it is assumed that the outcome is recorded, so that the system can always be described as a pure state. In this case we follow the quantum state through random sequence of outcomes, occurring with the probabilities such as those stated in Eqs. (18) and (26). The measurements introduce both non-linearity and randomness, with the former occurring due to the normalization in the probabilities, while the latter supplements the randomness from the unitary dynamics to which we turn now.

II. NOISY UNITARY DYNAMICS OF THE ISOLATED SYSTEM

We let the noisy dynamics unfold in eventually infinitesimally small time steps dt , indexed by a discrete time τ on the quantum state $|\psi_\tau\rangle \equiv |\psi(\tau dt)\rangle$. In the absence of measurements, the isolated system dynamics can therefore be written as

$$|\psi_{\tau+1}\rangle = U_\tau |\psi_\tau\rangle, \quad (36)$$

and hence is obtained from the time-evolution operator U_τ over the given time step, which is an $N \times N$ dimensional unitary matrix. Aiming at a statistical description of a noisy system, we introduce randomness into these dynamics by a standard random-matrix approach, mirroring Dyson's Brownian motion [34] and taking the general form of a Wiener process. In this section, we define this process in detail for the isolated system, and obtain the resulting statistics of the quantum state at long times. This recovers results connected to the circular unitary ensemble (CUE) of random-matrix theory, but adapted to the quantities of interest, and will serve as a benchmark for the monitored dynamics. Furthermore, discussing the isolated dynamics first allows us to introduce general methodology that we then can extend to the monitored case.

A. Wiener process

We generate the random noisy dynamics from time evolution operators that are close to the identity,

$$U_\tau = 1 + i\varepsilon H_\tau - \varepsilon^2/2 + O(\varepsilon^3), \quad (37)$$

where the dimensionless generators H_τ are taken independently from the Gaussian unitary ensemble (GUE), scaled so that in the ensemble average $\overline{H_\tau^2} = \mathbb{1}$. The generators then play the role of noise in a Wiener process, as quantified by the ensemble-averaged strength

$$\overline{|(U_\tau)_{nm}|^2} = \varepsilon^2/N \quad (38)$$

of the off-diagonal elements $n \neq m$. Consequently, the dynamics unfold on an effective time scale $t_\varepsilon = dt/\varepsilon^2$. Interpreted parametrically as a process sampling $U(n)$, hence considering the composed time-evolution operator $U = \prod_\tau U_\tau$ itself, this amounts to Dyson's Brownian motion process, a powerful tool to obtain statistical insights into the CUE whose Haar measure is approached in the stationary limit. This process is then conveniently studied using Fokker-Planck equations, as we set out here in terms of the quantum-state dynamics itself.

For a given set of statistical quantities $z_n = x, y, \dots$, the passage to the Fokker-Planck equation requires us to obtain the drift, diffusion, and cross-correlation coefficients

$$d_x \equiv \lim_{\varepsilon \rightarrow 0} \overline{\frac{x_{\tau+1} - x_\tau}{dt/t_\varepsilon}} \quad (39)$$

$$D_x \equiv \lim_{\varepsilon \rightarrow 0} \overline{\frac{(x_{\tau+1} - x_\tau)^2}{dt/t_\varepsilon}} \quad (40)$$

$$D_{x,y} \equiv \lim_{\varepsilon \rightarrow 0} \overline{\frac{(x_{\tau+1} - x_\tau)(y_{\tau+1} - y_\tau)}{dt/t_\varepsilon}}, \quad (41)$$

obtained from the ensemble-averaged first and second moments of the increments in order ε^2 . In analogy to our convention for the measurements, we express these coefficients again in terms of the initial data x_τ, y_τ, \dots (Ito calculus), and in the interest of compact notation then drop the time index τ . The corresponding Fokker-Planck equation takes the general form

$$\begin{aligned} \frac{\partial}{\partial t} P(\{z_k\}; t) &= - \sum_n \frac{\partial}{\partial z_n} d_{z_n} P(\{z_k\}; t) \\ &+ \frac{1}{2} \sum_{nm} \frac{\partial^2}{\partial z_n \partial z_m} D_{z_n, z_m} P(\{z_k\}; t), \end{aligned} \quad (42)$$

where we identify $D_{z_n, z_n} = D_{z_n}$. The stationarity statistics $P(\{z_k\}) = \lim_{t \rightarrow \infty} P(\{z_k\}; t)$ are then obtained from the stationarity condition $\frac{\partial}{\partial t} P(\{z_n\}; t) = 0$. We now apply this approach to systems with different numbers of qubits.

B. Noisy dynamics of a single qubit

For a system with a single qubit parameterized as in Eq. (3), we find the ensemble averages

$$d_r = 1/2 - r, \quad (43)$$

$$D_r = r(1 - r). \quad (44)$$

These give rise to the Fokker-Planck equation

$$\frac{\partial}{\partial t} P(r; t) = -t_\varepsilon^{-1} \frac{\partial}{\partial r} \left[\left(\frac{1}{2} - r - \frac{1}{2} \frac{\partial}{\partial r} r(1 - r) \right) P(r; t) \right] \quad (45)$$

for the time-dependent probability density $P(r; t)$. The transient dynamics depends on the initial distribution, which for instance may represent a random or a prescribed state. Here we focus on the emergent stationary behaviour at large times, which follows from the stationarity condition $\frac{\partial}{\partial t} P(r; t) = 0$. In the present setting, the resulting stationary distribution is uniform,

$$P(r) = 1 \quad (0 \leq r \leq 1). \quad (46)$$

Monitoring the system will modify this distribution due to the measuring backaction.

C. Noisy dynamics of multiple qubits

For systems of q qubits, with states parameterized as in Eq. (3), we similarly find

$$d_{r_n} = 1/N - r_n, \quad (47)$$

$$D_{r_n} = \frac{2}{N} r_n (1 - r_n), \quad (48)$$

$$D_{r_n, r_m} = -\frac{2}{N} r_n r_m, \quad (49)$$

with the cross-correlator in the last line applying to $n \neq m$. The expressions for each r_n close, so that their marginal distributions follow directly from the corresponding Fokker-Planck equation

$$\begin{aligned} \frac{\partial}{\partial t} P(r_n, t) &= \\ &- t_\varepsilon^{-1} \frac{\partial}{\partial r_n} \left[\left(\frac{1}{N} - r_n + \frac{1}{N} \frac{\partial}{\partial r_n} r_n (1 - r_n) \right) P(r_n, t) \right]. \end{aligned} \quad (50)$$

From the stationarity condition, these distribution are then found to be given by

$$P(r_n) = (N - 1)(1 - r_n)^{N-2} \quad (0 \leq r_n \leq 1). \quad (51)$$

These distributions are again independent of the initial conditions, and correspond to the known distributions of individual matrix elements in the CUE, which reflects the unitary invariance of this ensemble. This invariance will no longer hold true in the presence of monitoring, so that these distributions serve as a useful benchmark.

D. Two qubits and the role of constraints

For two qubits, the four probability coefficients r_n , $n = 1, 2, 3, 4$ follow the parabolic distribution

$$P(r_n) = 3(1 - r_n)^2 \quad (0 \leq r_n \leq 1). \quad (52)$$

The parameterization (9) for the state of two qubits leads to statistical quantities that are not naturally discussed in the context of CUE matrix statistics, even though they can be obtained from it (see Appendix B). For these quantities we find

$$\begin{aligned} d_r &= 1/2 - r, \\ d_R &= 1/2 - R, \\ d_C &= -3C/2 + (1/2 - r)(1/2 - R), \\ D_r &= r(1 - r)/2, \\ D_R &= R(1 - R)/2, \\ D_C &= [C(1 - 2r)(1 - 2R) - C^2 + r(1 - r)R(1 - R)]/2, \\ D_{r,R} &= C/2, \\ D_{r,C} &= (1/2 - r)C, \\ D_{R,C} &= (1/2 - R)C. \end{aligned} \quad (53)$$

These coefficients can again be introduced into a corresponding Fokker-Planck equation. Remarkably, as

$$\sum_{x \in \{r, R, C\}} \frac{\partial}{\partial x} d_x = \frac{1}{2} \sum_{x, y \in \{r, R, C\}} \frac{\partial^2}{\partial x \partial y} D_{x, y}, \quad (54)$$

the resulting stationary joint distribution of these quantities is still uniform, but is subject to nontrivial constraints on the domain of C :

$$\begin{aligned} P(r, R, C) = 6, \quad & \left(0 \leq r, R \leq 1 \text{ and} \right. \\ & - \min((1 - r)(1 - R), rR) < C \\ & \left. < \min(r(1 - R), R(1 - r)) \right). \end{aligned} \quad (55)$$

These constraints have a geometric interpretation, where they relate to extremal positions of state vectors of lengths r and R referring to parts of the quantum state where the first or second qubit is in state $|0\rangle$. When one integrates out the complementary variables, the constraints determine the integration domain, which leads to the marginal distributions

$$P(r) = 6r(1 - r) \quad (0 < r < 1), \quad (56)$$

$$P(R) = 6R(1 - R) \quad (0 < R < 1), \quad (57)$$

$$\begin{aligned} P(C) &= 6\sqrt{1 - 4|C|} - 24|C| \operatorname{atanh}(\sqrt{1 - 4|C|}) \\ & \quad (-1/4 < C < 1/4). \end{aligned} \quad (58)$$

As the drift and diffusion expressions for r and R again close individually, their marginal contributions can also be obtained directly from the corresponding Fokker-Planck equations, delivering the same results. We can

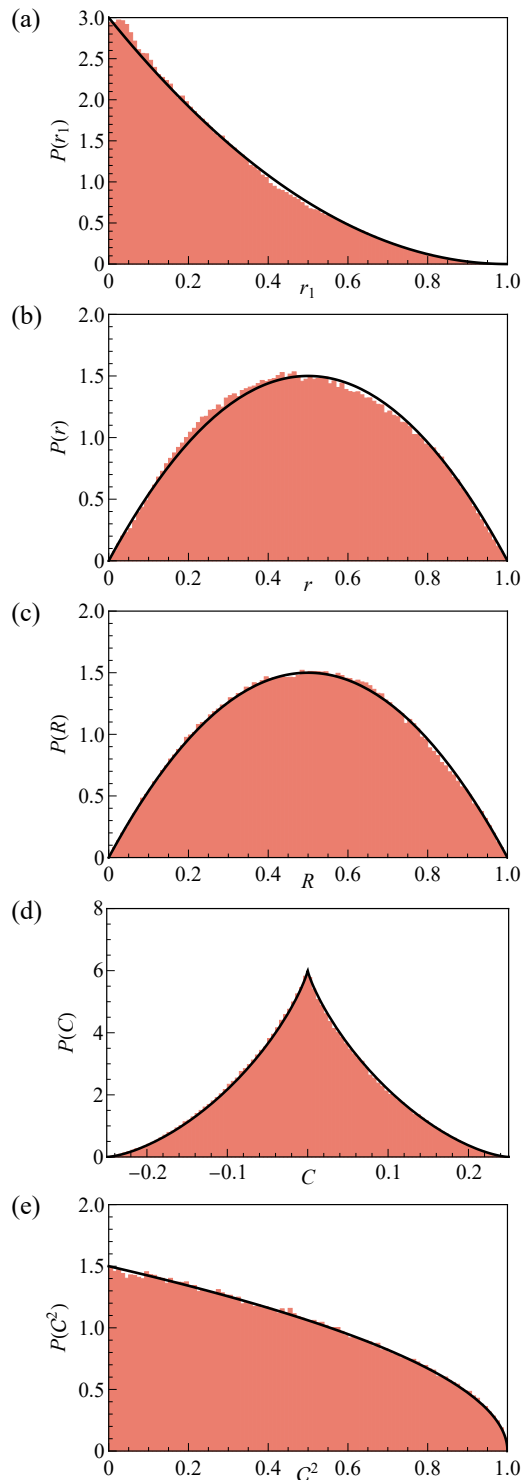


FIG. 1. For an isolated system of two qubits evolving under noisy unitary dynamics (36) generated by unitary operators (37), the panels compare analytical results (curves) for the stationary statistics of the quantum state to numerical data (histograms) from a single trajectory obtained for $\varepsilon = 0.1$. The statistical quantities and analytical results are (a) probability coefficient r_1 to find the qubits in state $|00\rangle$, Eq. (52), (b,c) probability coefficients r and R to find the first or second qubit in state $|0\rangle$, Eqs. (56,57), (d) correlation coefficient C , Eq. (58), and (e) squared concurrence C^2 , Eq. (62).

also write down the joint distribution of the two probability coefficients,

$$P(r, R) = 6 \min(r, R, 1-r, 1-R), \quad (0 \leq r, R \leq 1). \quad (59)$$

Furthermore, we find that the equations for the concurrence \mathcal{C} also close,

$$d_{\mathcal{C}} = \frac{1}{4\mathcal{C}} - \mathcal{C}, \quad (60)$$

$$D_{\mathcal{C}} = \frac{1}{2}(1 - \mathcal{C}^2). \quad (61)$$

This results in the distribution

$$P(\mathcal{C}) = 3\mathcal{C}\sqrt{1 - \mathcal{C}^2}, \quad (62)$$

or, equivalently

$$P(\mathcal{C}^2) = \frac{3}{2}\sqrt{1 - \mathcal{C}^2}. \quad (63)$$

In Figure 1, these analytical results are compared to numerical results. While for the present case of isolated unitary dynamics such data could be obtained by directly sampling the CUE, this would not extend to the case of monitored dynamics. Therefore, we base the numerics on the discretised stochastic time evolution (36), generated by unitary operators (37) with $\varepsilon = 0.1$. The data in Figure 1 is then obtained from the states along a single trajectory, of length 5×10^5 time steps. This results in good agreement, which we next aim to replicate for monitored dynamics. This will also guide us to a more general understanding of geometric constraints such encountered in Eq. (55).

III. DYNAMICS MONITORED BY A SINGLE DESIGNATED QUBIT

We now combine the noisy unitary dynamics with continuous monitoring, following a protocol where each unitary step of the time evolution is supplemented by a variable-strength measurement, both considered over an infinitesimally small time step. As the noise in these two stochastic processes is mutually uncorrelated, they can be combined into a single process in which drift, diffusion, and cross-correlation coefficients sum up. Maintaining the definitions (39), (40), and (41) of these coefficients including their scaling with t_ε , the dynamics are then governed by a dimensionless monitoring strength $\Lambda = \lambda^2/\varepsilon^2$. This allows us again to formulate Fokker Planck equations for the quantities of interest, which we can study in the stationary limit. In the present section, we carry out this program for the case of a system in which one designated qubit is monitored.

A. Single-qubit system

We start with the simplest case, in which the monitored qubit is the only qubit in the system. Combining

the noisy unitary dynamics with continuous monitoring of this qubit, the probability coefficient r obtains the drift and diffusion coefficients

$$d_r = 1/2 - r, \quad (64)$$

$$D_r = r(1 - r) + 4\Lambda r^2(1 - r^2). \quad (65)$$

This gives the joint distribution

$$P(r) = \frac{c_\Lambda}{(1 + 4\Lambda r(1 - r))^2}, \quad (66)$$

where c_Λ is for normalization. We see that the monitoring induces a bimodal character to this distribution, which becomes concentrated at $r = 0$ and $r = 1$ as the effective monitoring strength Λ increases. Physically, this can be interpreted as a signature of the measurement backaction.

B. Monitoring of one of two qubits

We next apply these considerations to a system of two qubits, where the first one is designated to be monitored. This situation is usefully studied in the parameterization (9), where we obtain

$$\begin{aligned} d_r &= d_r^{(0)}, \\ d_R &= d_R^{(0)}, \\ d_{\mathcal{C}} &= d_{\mathcal{C}}^{(0)} - 4\Lambda Cr(1 - r), \\ D_r &= D_r^{(0)} + 4\Lambda r^2(1 - r)^2, \\ D_R &= D_R^{(0)} + 4\Lambda C^2, \\ D_{\mathcal{C}} &= D_{\mathcal{C}}^{(0)} + 4\Lambda C^2(1 - 2r)^2, \\ D_{r,R} &= D_{r,R}^{(0)} + 4\Lambda Cr(1 - r), \\ D_{r,C} &= D_{r,C}^{(0)} + 4\Lambda Cr(1 - r)(1 - 2r), \\ D_{R,C} &= D_{R,C}^{(0)} + 4\Lambda C^2(1 - 2r). \end{aligned} \quad (67)$$

Here, the quantities with superscript (0) refer to the expressions without monitoring, given in Eq. (53).

From this, we find that subject to the same constraints as given in Eq. (55), the joint distribution only explicitly depends on r ,

$$P(r, R, C) = c_\Lambda \frac{1}{(1 + 8\Lambda r(1 - r))^3}. \quad (68)$$

This allows us to obtain closed analytical expressions for the marginal distributions of these quantities, as well as the individual quantities r_n , and the concurrence \mathcal{C} . In particular, for the coefficient r , this gives the marginal distribution

$$P(r) = c_\Lambda \frac{r(1 - r)}{(1 + 8\Lambda r(1 - r))^3}. \quad (69)$$

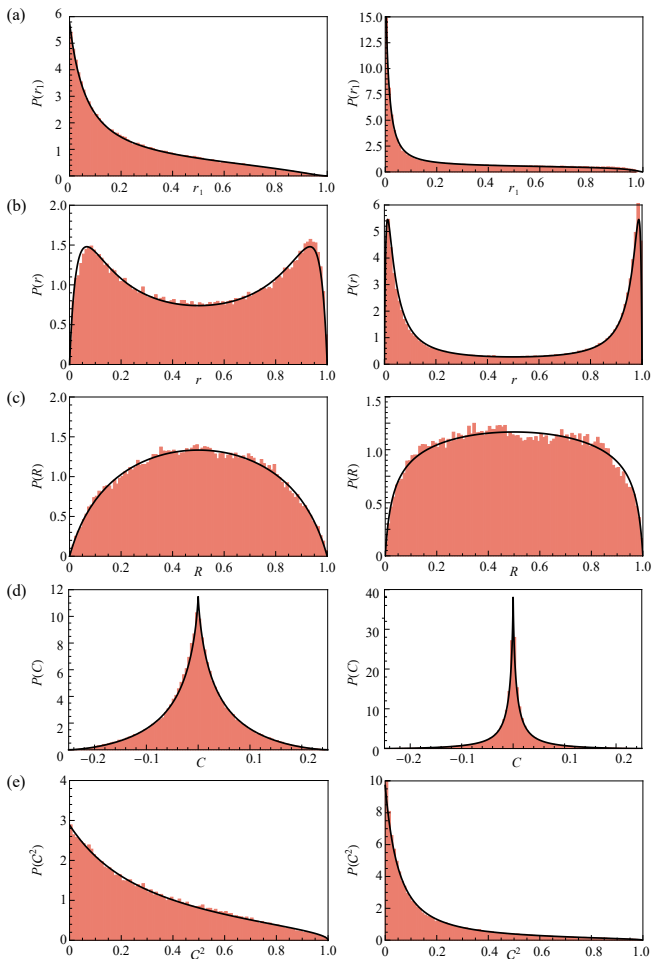


FIG. 2. Stationary quantum state statistics in a system of two qubits, where the first qubit is monitored with effective strength $\Lambda = 1$ (left column) or $\Lambda = 5$ (right column). The different panels address the same quantities as in Fig. 1, and the numerical data is obtained in an analogous way, but with measurements of strength $\lambda = 0.1$ (left column) or $\lambda = \sqrt{0.05}$ (right column) carried out after each unitary step. The curves represent the analytical expressions from Sec. III B and Appendix C.

For the other quantities, highly nontrivial distributions arise as they depend on r via the constraints, which is reflected by unwieldy formulas that we present in Appendix C.

In Fig. 2, these analytical results are compared to numerical results in a discretised stochastic time evolution with $\varepsilon = 0.1$. In analogy to Fig. 1, the data is obtained from single quantum trajectories, but now with each unitary time step followed by a variable strength measurement as described in Sec. I B 2. We fix the microscopic measurement strength to $\lambda = 0.1$ and $\lambda = \sqrt{0.05} \approx 0.224$, corresponding to effective measurement strengths $\Lambda = 1$ and $\Lambda = 5$. As for the case without monitoring, we find good agreement, including for the probability coefficients r and R of the monitored and unmonitored qubits,

which now follow different statistics.

We see that as the measurement strength increases, $P(r)$ again develops a bimodal shape peaked at $r = 0$ and $r = 1$, approaching the case of a hard projective measurement. In parallel, the distribution $P(R)$ flattens out, slowly approaching the constant form of a single isolated qubit, while $P(C)$ become increasingly more confined to the regions of vanishing classical correlations ($C = 0$), and $P(C^2)$ replicates this as a trend towards vanishing quantum correlations ($C^2 = 0$).

C. Monitoring one of q qubits

For a larger collection of q qubits, of which the first is monitored, we obtain the drift, diffusion, and cross-correlation coefficients

$$d_{r_n} = \frac{1}{N} \left(\sum_{m \neq n} r_m - (N-1)r_n \right), \quad (70)$$

$$D_{r_n} = \frac{2}{N} r_n \sum_{m \neq n} r_m + 4\Lambda r_n^2 (r + x_n - 1)^2, \quad (71)$$

$$D_{r_n, r_m} = -\frac{2}{N} r_n r_m + 4\Lambda r_n r_m (r + x_n - 1)(r + x_m - 1). \quad (72)$$

Here $x_n = 0$ for all indices $n \leq N/2$ in which the monitored qubit is in state $|0\rangle$ and $x_n = 1$ when it is in state $|1\rangle$, while $r = \sum_{n|x_n=0} r_n$ is the probability coefficient of the monitored qubit, as already introduced in Eq. 12. These relations imply that the joint distribution of the probability coefficients is a function only of r ,

$$P(\{r_n\}) = \frac{c_\Lambda}{(1 + 2N\Lambda r(1-r))^{N/2-1}} \delta\left(\sum_n r_n - 1\right) \quad (73)$$

with suitable normalization constant c_Λ , capturing the constraints now via an over-parametrization in a delta function. Indeed the equations for this coefficient continue to close, giving

$$d_r = \frac{1}{2} - r, \quad (74)$$

$$D_r = \frac{2}{N} r(1-r) + 4\Lambda r^2(1-r^2). \quad (75)$$

From this, we obtain the marginal distribution

$$P(r) = c_\Lambda \frac{[(1-r)r]^{(N/2)-1}}{(1 + 2N\Lambda(1-r)r)^{(N/2)+1}}. \quad (76)$$

This once more agrees very well with numerical simulations of the dynamics, as shown for a system of size $q = 4$ in Fig. 3. Furthermore, we then obtain the statistics of other properties of the states by combining this with the geometric constraint, allowing us to express their probability distributions in terms of integrals. In Fig. 3, we illustrate this for the probability distribution

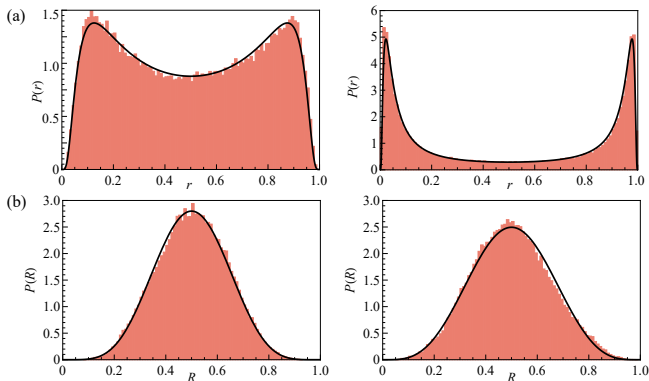


FIG. 3. Monitoring one of four qubits. The panels show the probability densities of the probability coefficients r of a designated monitored qubit and R of one of the unmonitored qubits, for effective monitoring strength $\Lambda = 1$ (left column) and $\Lambda = 5$ (right column). The numerical data is obtained via the same process as underlying Fig. 2, the analytical result for $P(r)$ is given by Eq. (76), while the result for $P(R)$ follows by combining this with the geometric constraints in the form of Eq. (77).

of the summed probability coefficient R of one of the non-monitored quantum bits. For this, the analytical prediction arises by writing

$$R_m = r\tilde{r}_0 + (1-r)\tilde{r}_1, \quad (77)$$

where r is distributed according to Eq. (76), and \tilde{r}_0, \tilde{r}_1 independently follow the same distribution but with $\Lambda \rightarrow 0, N \rightarrow N/2$. This again corresponds to a picture where the monitoring conditions the statistics of r , which then transfers to other statistical properties via geometric constraints.

IV. MONITORING SEVERAL QUBITS

Following the principles and procedure outlined in the previous section, we can also formulate the noisy dynamics of systems in which multiple quantum bits are monitored. For the example of monitoring two quantum bits with effective strengths Λ and Λ' , this amends the drift, diffusion, and cross-correlation coefficients in Eq. (67), to

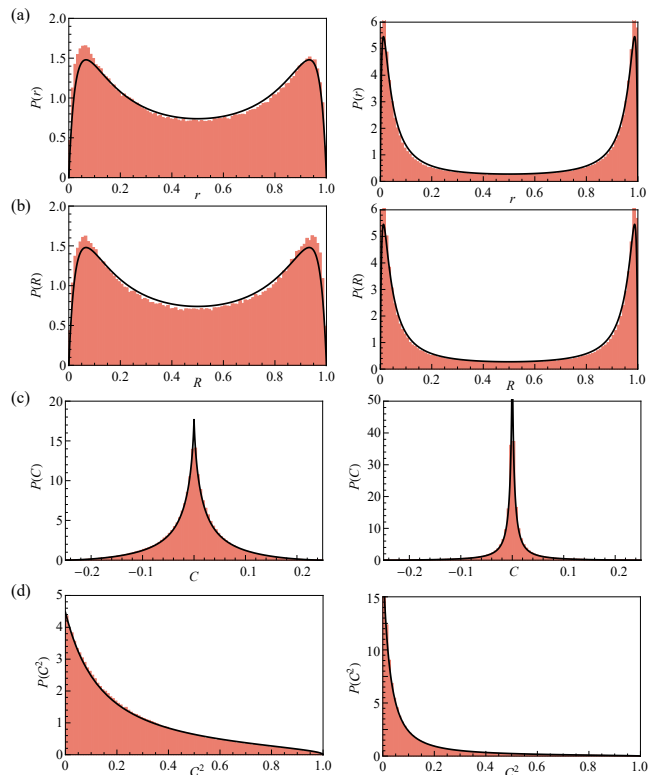


FIG. 4. The numerical data shows the stationary quantum state statistics in a system of two qubits, where both are monitored with equal strength $\Lambda = \Lambda' = 1$ (left column) or $\Lambda = \Lambda' = 5$ (right column). In this case, the curves are not exact analytical predictions, but capture the phenomenological observation that these results bear similarities to distributions in the system where just one of the two qubits is monitored, with suitable identifications of distributions and effective monitoring strengths as described in the text.

which we now refer with a superscript (1), to read

$$\begin{aligned} d_r &= d_r^{(1)}, \\ d_R &= d_R^{(1)}, \\ d_C &= d_C^{(1)} - 4\Lambda'CR(1-R), \\ D_r &= D_r^{(1)} + 4\Lambda'C^2, \\ D_R &= D_R^{(1)} + 4\Lambda'R^2(1-R)^2, \\ D_C &= D_C^{(1)} + 4\Lambda'C^2(1-2R)^2, \\ D_{r,R} &= D_{r,R}^{(1)} + 4\Lambda'CR(1-R), \\ D_{r,C} &= D_{r,C}^{(1)} + 4\Lambda'C^2(1-2R), \\ D_{R,C} &= D_{R,C}^{(1)} + 4\Lambda'CR(1-R)(1-2R). \end{aligned} \quad (78)$$

While we then can formulate stationarity conditions that determine the joint probability distribution of the quantities at large times, these are not easily solved. Therefore, we here illustrate the resulting statistics based on numerical results.

In Fig. 4, we show the marginal distributions of r , R , C and C^2 for various combinations of $\Lambda = \Lambda' = 1$ and $\Lambda = \Lambda' = 5$. We then make the phenomenological observation that the distributions are similar to the distributions in a system with just a single monitored qubit, Sec. III B, with the following identifications. The probability densities $P(r) = P(R)$ are close to Eq. (69), at $\Lambda_{\text{eff}} = \Lambda = \Lambda'$. On the other hand, the probability densities for C and C^2 are close to Eqs. (C3) and (C6), but with $\Lambda_{\text{eff}} = \Lambda + \Lambda'$.

V. APPLICATION TO A MONITORED KICKED TOP

To round of this study, we consider monitoring in a deterministic system in which the noisy dynamics reflect the quantum signatures of chaos. For this, we choose the kicked top [33], the dynamics of angular momentum (J_x, J_y, J_z) obtained from a Floquet operator

$$F = F_x F_y, \quad (79)$$

$$F_x = \exp\left(-i \frac{k}{2j+1} J_x^2 - i\beta_x J_x\right)$$

$$F_y = \exp(-i\beta_y J_y) \quad (80)$$

that combines rotations by angles β_x and β_y with a torsion of strength k . This system is a paradigm of complex quantum dynamics, inherited from a classical limit that turns chaotic at large enough torsion strength. This classical limit is attained when the angular quantum number j becomes large.

We set $\beta_x = 0.8$, $\beta_y = 2$, $k = 8$, $j = 15/2$ ($N = 2j+1 = 16$), and slice each of the two factors F_x and F_y in the time evolution up into n_T steps, between which we insert variable-strength measurement operations detecting whether the state is in the upper or lower hemisphere in the J_z eigenbasis. This monitoring has just two possible outcomes with equal degeneracy, hence, with our choice of j , is equivalent to monitoring a designated qubit in a four-qubit system. We then compare the statistics of a single quantum trajectory over $> 10^5$ sliced time steps with the analytical results for this scenario in the stochastic model, where we set the effective monitoring strength to the natural value $\Lambda = \lambda^2 n_T$ and keep $\lambda = 0.1$ fixed.

We then identify two regimes. As shown in Fig. 5, for $n_T = 10$ and $n_T = 20$, where the corresponding $\Lambda = 0.1, 0.2$ is small, the results from the monitored kicked top are in acceptable agreement with the stochastic model, as captured in the analytical results of Sec. III C. This is the regime where the alternating factors F_x and F_y mimic noise on time scales shorter than the monitoring time scale, which washes out any potential differences in the dynamical time scales of the two factors.

However, as shown in Fig. 6, for the larger value $\Lambda = 0.4$ the results from the monitored kicked top deviate from the stochastic model. Indeed, in this regime we obtain distinct statistics at the end of the rotation F_y and at the end of the torsion F_x . Each of these statistics

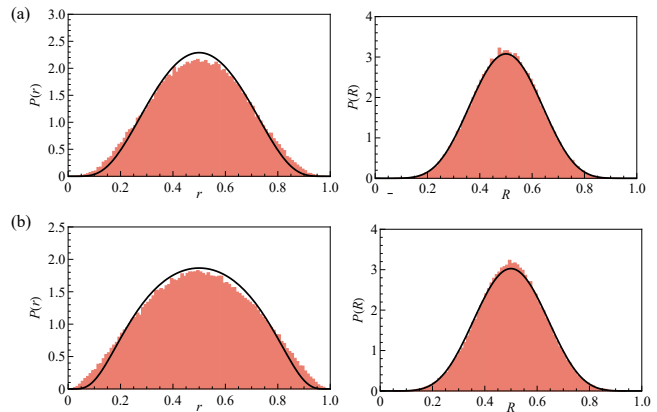


FIG. 5. Comparison of numerical data for a monitored kicked top in the regime of weak monitoring, with $\lambda = 0.1$ and (a) $n_T = 10$ or (b) $n_T = 20$ (for further details see text), to the analytical results in the equivalent setting of a noisy quantum circuit with (a) $\Lambda = 0.1$ or (b) $\Lambda = 0.2$.

resembles, at least qualitatively, the data in the stochastic model at suitable effective strength $\Lambda_{\text{rot}} \approx 0.2 = 2\Lambda$ and $\Lambda_{\text{tor}} \approx 0.8 = \Lambda/2$, which can be interpreted as reflecting different levels of dynamical noise in F_x and F_y that are resolved by the monitoring. This demonstrates that the stochastic description developed in this work can be usefully applied to settings well outside the domain it has been initially defined, and then gives illuminating insights into the monitored dynamics of generic complex quantum systems.

VI. CONCLUSIONS

In summary, in this work I formulated stochastic processes representing the noisy dynamics of monitored multi-qubit systems, and used these to describe the quasistationary statistics of the quantum state attained at long times. For the case of monitoring a single designated qubit in the system, this yields exact analytical descriptions in terms of the probability coefficients of the state. This leads to an understanding of the role of classical and quantum correlations in mediating the effects of monitoring. In a statistical interpretation, the monitoring conditions the state of the monitored qubit, which then translates into nontrivial statistics of the other qubits via geometric constraints. On the dynamical level, this indirect effect of the monitoring is mediated by correlations, such as the parameter embodied C that I introduced to parameterise two-qubit states. These indirect effects also occur in more complicated setting where multiple qubits are monitored at different strengths, which we illustrated by numerical results complementing our analytical considerations. Furthermore, the results obtained here also serve as a benchmark for monitoring in deterministic systems displaying the quantum signatures of chaos, as I illustrated for the quantum kicked top.

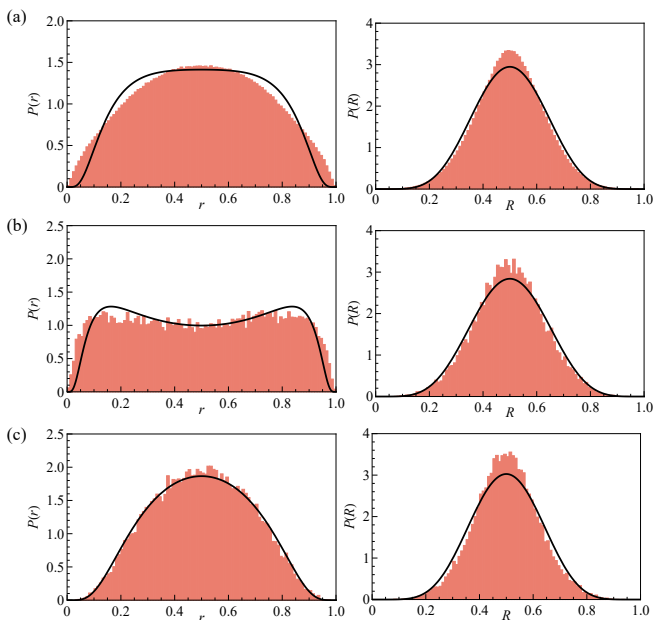


FIG. 6. Comparison of numerical data for a monitored kicked top at stronger monitoring, with $\lambda = 0.1$ and $n_T = 40$, recorded (a) at all time steps, (b) at the end of the rotation, and (c) at the end of the torsion, to the analytical results in the equivalent setting of a noisy quantum circuit with (a) $\Lambda = 0.4$, (b) $\Lambda = 0.8$, and (c) $\Lambda = 0.2$.

A specific open random-matrix problem arising from this work is to solve the case of multiple monitored qubits analytically. The framework described here allows to formulate the corresponding Fokker-Planck equations, but in these, the drift and diffusion coefficients then do no longer follow a hierarchical pattern, as is apparent when comparing the minimal case of two qubits, Eqs. (67) and (78). A solution of the general case may still be possible by a suitable extension of the parametrisation (7), which in itself appears to be a worthwhile task for its utility to extract statistical correlations and interpret the results physically and mathematical in terms of geometric constraints. For instance, it may well be possible to then formulate such constraints via a maximal-entropy principle, and identify the common statistical ground for the mathematically intriguing probability distributions that appear in this work.

Furthermore, a distinguishing feature of the noisy dynamics that we considered here is that these act globally on the complete system, mirroring the dynamics in a fully ergodic many-body quantum system. Indeed, we formulated the dynamics akin to Dyson's Brownian-motion process, which efficiently captures the statistics of such systems in a random-matrix description, even though here this took the form of random *states*. On the other hand, the measurement protocol employed in the monitoring extracts local information from the system. This work can therefore be extended in various directions. Amongst these, a particularly interesting case is

that of quantum circuits built out of two-qubit gates that act locally. As mentioned in the introduction, these display a transition in the entanglement characteristics as the monitoring strength is increased, which was first realized in a stroboscopic setting, but also applies to continuously monitored noisy dynamics. Another variation is to consider the statistics for post selected dynamics, hence, the conditional probabilities obtained for a given, fixed, sequence of measurement outcomes. Conversely, the dynamics can be averaged incoherently over such outcomes, which captures decoherence in an open-system setting. Furthermore, we can extend the considerations to physical components encompassing more than two levels, and again include deterministic systems in which the noisy dynamics reflect the quantum signatures of chaos, as we already did for a single such component in Sec. (V). In these settings, one can adopt the generalised monitoring protocol in Appendix A, which can also be extended to describe monitoring of different, possibly nonlocal, observables. This raises the hope that the methods and findings presented in this paper inform the study of such systems, too.

ACKNOWLEDGMENTS

This paper is dedicated to my dearly loved and respected Doktorvater, Fritz Haake. The measurement process, random-matrix theory, and complex quantum systems displaying the signatures of underlying classical chaos are central themes in Fritzens Lebenswerk, which continues to inspire. I also thank Tara Kalsi and Alessandro Romito for fruitful discussions that helped to shape the precise incarnation of these themes in this work.

All numerical data in this work was directly obtained, processed, and plotted in Mathematica, making use of its implementation of Gaussian unitary ensembles and the Wigner D function. This data is therefore completely represented by the figures.

Appendix A: General version of the measurement protocol

For a general system of Hilbert-space dimension N , we formulate the variable-strength measurement protocol in terms of a set of measurement parameters $\{\lambda_n\}_{n=1}^N$, each characterizing the strength by which the different basis states are probed. This is achieved by controlled entanglement with an auxiliary system that has the same dimensionality, and then is measured.

1. Entanglement step

Initially, the joint system is in a separable state,

$$|\varphi\rangle = |\psi\rangle \otimes |0\rangle, \quad (\text{A1})$$

where $|0\rangle$ is a suitable state of the auxiliary system. The entanglement step takes this into the state

$$|\varphi\rangle = \sum_{n=1}^N \psi_n |n\rangle \otimes |\lambda_n\rangle, \quad (\text{A2})$$

where we set

$$|\lambda_n\rangle = \sum_{m=1}^N \sqrt{\frac{1-\lambda_n}{N} + \lambda_n \delta_{nm}} |m\rangle \quad (\text{A3})$$

(note the dual role played by the index n in this definition). This systematically enhances one of the amplitudes of the auxiliary system in correspondence with a partner basis state of the system.

2. Measurement step

Measuring the auxiliary system then results in outcomes $M = 1, 2, \dots, N$, which collapse the system state onto

$$|\psi_M\rangle = P_M^{-1/2} |\Psi_M\rangle, \quad (\text{A4})$$

$$|\Psi_M\rangle = \sum_{n=1}^N \sqrt{\frac{1-\lambda_n}{N} + \lambda_n \delta_{nM}} \psi_n |n\rangle, \quad (\text{A5})$$

$$\begin{aligned} P_M &= \langle \Psi_M | \Psi_M \rangle = \lambda_M |\psi_M|^2 + \sum_n \frac{1-\lambda_n}{N} |\psi_n|^2 \\ &= \frac{1}{N} + \lambda_M |\psi_M|^2 - \sum_n \frac{\lambda_n}{N} |\psi_n|^2, \end{aligned} \quad (\text{A6})$$

where P_M is the probability of the measurement outcomes. This sends the coefficients $r_{\tau-,n}$ to

$$r_{\tau+,n} = r_{\tau-,n} \frac{1-\lambda_n + N\lambda_n \delta_{nM}}{1 + N\lambda_M r_{\tau-,M} - \sum_m \lambda_m r_{\tau-,m}} \quad (\text{A7})$$

$$= r_{\tau-,n} + r_{\tau-,n} \frac{\sum_m \lambda_m (1-\delta_{mM})(r_{\tau-,m} - \delta_{nm})}{1 - \sum_m \lambda_m (1-\delta_{mM}) r_{\tau-,m}} \quad (\text{A8})$$

Averaged over the measurement outcomes, we always have $\overline{r_{\tau+,n}} = r_{\tau-,n}$.

3. Weak-measurement limit

If the measurement strengths $\{\lambda_n\}$ are all small, we obtain a weak measurement, in which the change of the coefficients can be approximated as

$$dr_{\tau,n} \equiv r_{\tau+,n} - r_{\tau-,n} \quad (\text{A9})$$

$$\begin{aligned} &= r_n \sum_m \lambda_m (1 - N\delta_{mM})(r_m - \delta_{nm}) \\ &\left(1 + \sum_m \lambda_m (1 - N\delta_{mM}) r_m \right) + O(\lambda^3) \end{aligned} \quad (\text{A10})$$

Averaged over the measurement outcomes, we then have

$$\overline{dr_{\tau,n}} = 0, \quad (\text{A11})$$

$$\begin{aligned} \overline{dr_{\tau,n} dr_{\tau,m}} &= r_n r_m \left[N \sum_{l=1}^N (r_l - \delta_{nl})(r_l - \delta_{ml}) \lambda_l^2 \right. \\ &\quad \left. - \sum_{l=1}^N (r_l - \delta_{nl}) \lambda_l \sum_{l=1}^N (r_l - \delta_{ml}) \lambda_l \right]. \end{aligned} \quad (\text{A12})$$

where the latter expression also applies for $n = m$.

Appendix B: Direct derivation of the joint distribution of r , R and C

Here we give a direct derivation of the uniform joint distribution $P(r, R, C)$, Eq. (55), of a completely random two-qubit state parametrised according to Eq. (9). We denote $(|\alpha|^2, |\beta|^2, |\gamma|^2, |\delta|^2) = (r_1, r_2, r_3, r_4)$ in accordance to Eq. (1), but momentarily lift the normalization of the state. This gives rise to the amended parametrization

$$r_1 = \mathcal{N}[C + rR], \quad r_2 = \mathcal{N}[r(1-R) - C], \quad (\text{B1})$$

$$r_3 = \mathcal{N}[R(1-r) - C], \quad r_4 = \mathcal{N}[(1-r)(1-R) + C], \quad (\text{B2})$$

corresponding to setting

$$r = \frac{r_1 + r_2}{(r_1 + r_2 + r_3 + r_4)}, \quad (\text{B3})$$

$$R = \frac{r_1 + r_3}{(r_1 + r_2 + r_3 + r_4)}, \quad (\text{B4})$$

$$C = \frac{r_1 r_4 - r_2 r_3}{(r_1 + r_2 + r_3 + r_4)^2}, \quad (\text{B5})$$

$$\mathcal{N} = r_1 + r_2 + r_3 + r_4, \quad (\text{B6})$$

including the additional normalization parameter \mathcal{N} .

The Jacobian of the transformation is

$$J = \left| \det \frac{\partial(r_1, r_2, r_3, r_4)}{\partial(r, R, C, \mathcal{N})} \right| = \mathcal{N}^3. \quad (\text{B7})$$

We then adopt any suitable distribution of the complex amplitudes ψ_n , such as the Gaussian distribution

$$P(\{\psi_n\}) = \exp\left(-\sum_{n=1}^4 |\psi_n|^2\right) / \pi^4, \quad (\text{B8})$$

that correctly reproduces the isotropic distribution of a normalized state when constrained to $\mathcal{N} = 1$. Integrating out the complex phases, the distribution indeed only depends on the normalization parameter, such as here

$$P(\{r_n\}) = \exp\left(-\sum_{n=1}^4 r_n\right). \quad (\text{B9})$$

Transformed to the new parameters, we then find

$$P(r, R, C, \mathcal{N}) = 6 \Theta(r, R, C) \times \frac{\mathcal{N}^3}{6} \exp(-\mathcal{N}), \quad (\text{B10})$$

where

$$\begin{aligned} \Theta(r, R, C) &= \Theta[C + rR] \times \Theta[-C + r(1 - R)] \\ &\times \Theta[-C + (1 - r)R] \times \Theta[C + (1 - r)(1 - R)] \\ &\times \Theta[r] \times \Theta[1 - r] \times \Theta[R] \times \Theta[1 - R] \end{aligned} \quad (\text{B11})$$

embodies the constraints on the parameters in terms of the unit step function $\Theta[\cdot]$. Importantly, these constraints are also independent of \mathcal{N} . Therefore, for any value of the normalization parameter, the distribution $P(r, R, C) = 6\Theta(r, R, C)$ is uniform, including for the normalized case $\mathcal{N} = 1$.

Appendix C: Explicit form of the analytical marginal distributions for monitoring one of two qubits

Here, we collect the explicit analytical expressions of marginal distributions for monitoring one of two qubits, discussed in subsection III B. This is based on the joint distribution (68) for r , R , and C , subject to constraints in (55), as well as reinterpretations of these constraints in equivalent geometric terms.

First, we integrate out any two of these quantities subject to the stated constraints. This entails the marginal distributions of the remaining quantity,

$$P(r) = c_\Lambda \frac{r(1-r)}{(1+8\Lambda r(1-r))^3}, \quad (\text{C1})$$

$$P(R) = c_\Lambda \left(\frac{8R(1-R)}{1+8\Lambda R(1-R)} + \frac{6}{\sqrt{2\Lambda}(2\Lambda+1)^{3/2}} \left[\operatorname{asinh}(\sqrt{2\Lambda}) + (2R-1) \operatorname{atanh} \left(\sqrt{\frac{2\Lambda}{2\Lambda+1}}(1-2R) \right) \right] \right) \quad (\text{C2})$$

$$\begin{aligned} P(C) &= c_\Lambda \frac{4\sqrt{1-4|C|} (64\Lambda^2|C| + \Lambda(56|C| + 4) + 5)}{(2\Lambda+1)(8\Lambda|C|+1)} \\ &+ c_\Lambda \frac{2\sqrt{2} (8\Lambda(32\Lambda^2 + 40\Lambda + 15)|C| + 3) \operatorname{atanh} \left(\sqrt{\frac{\Lambda(2-8|C|)}{2\Lambda+1}} \right)}{\sqrt{\Lambda}(2\Lambda+1)^{3/2}} - c_\Lambda(2\Lambda+1)128|C| \operatorname{atanh} \left(\sqrt{1-4|C|} \right). \end{aligned} \quad (\text{C3})$$

In all these expressions, c_Λ is a suitable normalization constant. Compared to the joint distribution (68), the marginally distributions are distinctively more nontrivial, and this is enforced by the constraints in Eq. (55).

This is useful as these constraints can be recovered in an equivalent picture, from which we can infer further statistics of the state. In this picture, the conditional states $|\tilde{\psi}_0\rangle$ and $|\tilde{\psi}_1\rangle$ of the second qubit, where the monitored qubit is in state $|0\rangle$ or $|1\rangle$, are uncorrelated, while their lengths are again conditioned by the probability coefficient r . Therefore,

$$\langle \tilde{\psi}_0 | \tilde{\psi}_0 \rangle = r, \quad \langle \tilde{\psi}_1 | \tilde{\psi}_1 \rangle = 1 - r, |\langle \tilde{\psi}_0 | \tilde{\psi}_1 \rangle|^2 = r(1-r)x, \quad (\text{C4})$$

where x is then uniformly distributed in $[0, 1]$, independently of x . In terms of this data, the squared concurrence takes the form

$$\mathcal{C}^2 = 4r(1-r)(1-x). \quad (\text{C5})$$

From this, we can derive the corresponding probability distribution,

$$P(\mathcal{C}^2) = \frac{c'_\Lambda}{(2\mathcal{C}^2\Lambda+1)^2} \left(4((6\mathcal{C}^2+4)\Lambda+5)\sqrt{(1-\mathcal{C}^2)\Lambda(2\Lambda+1)} + 6\sqrt{2}(2\mathcal{C}^2\Lambda+1)^2 \operatorname{atanh} \left(\sqrt{\frac{(1-\mathcal{C}^2)2\Lambda}{2\Lambda+1}} \right) \right) \quad (\text{C6})$$

with $c'_\Lambda = c_\Lambda/[128\sqrt{\Lambda}(2\Lambda+1)^{5/2}]$.

Analogously we can interpret each of the components of the subvectors as random, and hence write $r_1 = x'r$ where

$0 \leq x' \leq 1$, again with a uniform distribution. This gives

$$P(r_n) = \frac{c'_\Lambda}{(1 - 8\Lambda(r_n - 1)r_n)^2} \left[8\sqrt{\Lambda(2\Lambda + 1)}(r_n - 1)[-5 + 8r_n + (32r_n^2(1 - \Lambda) - 4(6r_n + 1))(1 - r_n)\Lambda] \right. \\ \left. + 6\sqrt{2} \operatorname{asinh}(\sqrt{2\Lambda}) (1 - 8\Lambda(r_n - 1)r_n)^2 + 6\sqrt{2}(1 - 8\Lambda(r_n - 1)r_n)^2 \operatorname{atanh}\left(\frac{1 - 2r_n}{\sqrt{\frac{1}{2\Lambda} + 1}}\right) \right]. \quad (\text{C7})$$

These nontrivial distributions again combine the monitoring-conditioned statistics of the parameter r with suitable r -dependent constraints.

-
- [1] J. von Neumann, *Mathematical Foundation of Quantum Theory* (Princeton University Press, Princeton, NJ, 1938).
- [2] H. M. Wiseman and G. J. Milburn, *Quantum Measurement and Control* (Cambridge University Press, Cambridge, 2009).
- [3] K. Jacobs, *Quantum Measurement Theory and its Applications* (Cambridge University Press, 2014).
- [4] F. Haake, Statistical treatment of open systems by generalized master equations, in *Springer tracts in modern physics* (Springer, 1973) pp. 98–168.
- [5] S. Gnutzmann, T. Guhr, H. Schomerus, and K. Życzkowski, Special issue in honour of the life and work of Fritz Haake, *J. Phys. A* **54**, 130301 (2021).
- [6] H. Carmichael, *An Open Systems Approach to Quantum Optics: Lectures Presented at the Université Libre de Bruxelles, October 28 to November 4, 1991*, Lecture Notes in Physics Monographs (Springer Berlin Heidelberg, 2009).
- [7] A. Chan, R. M. Nandkishore, M. Pretko, and G. Smith, Unitary-projective entanglement dynamics, *Phys. Rev. B* **99**, 224307 (2019).
- [8] B. Skinner, J. Ruhman, and A. Nahum, Measurement-induced phase transitions in the dynamics of entanglement, *Phys. Rev. X* **9**, 031009 (2019).
- [9] Y. Li, X. Chen, and M. P. A. Fisher, Quantum Zeno effect and the many-body entanglement transition, *Phys. Rev. B* **98**, 205136 (2018).
- [10] Y. Li, X. Chen, and M. P. A. Fisher, Measurement-driven entanglement transition in hybrid quantum circuits, *Phys. Rev. B* **100**, 134306 (2019).
- [11] Y. Li and M. P. A. Fisher, Statistical mechanics of quantum error correcting codes, *Phys. Rev. B* **103**, 104306 (2021).
- [12] M. J. Gullans and D. A. Huse, Dynamical purification phase transition induced by quantum measurements, *Phys. Rev. X* **10**, 041020 (2020).
- [13] M. J. Gullans and D. A. Huse, Scalable probes of measurement-induced criticality, *Phys. Rev. Lett.* **125**, 070606 (2020).
- [14] A. Zabalo, M. J. Gullans, J. H. Wilson, S. Gopalakrishnan, D. A. Huse, and J. H. Pixley, Critical properties of the measurement-induced transition in random quantum circuits, *Phys. Rev. B* **101**, 060301 (2020).
- [15] O. Lunt, M. Sznyszewski, and A. Pal, Measurement-induced criticality and entanglement clusters: A study of one-dimensional and two-dimensional Clifford circuits, *Phys. Rev. B* **104**, 155111 (2021).
- [16] A. Zabalo, M. J. Gullans, J. H. Wilson, R. Vasseur, A. W. W. Ludwig, S. Gopalakrishnan, D. A. Huse, and J. H. Pixley, Operator scaling dimensions and multifractality at measurement-induced transitions, *Phys. Rev. Lett.* **128**, 050602 (2022).
- [17] Y. Li, X. Chen, A. W. W. Ludwig, and M. P. A. Fisher, Conformal invariance and quantum nonlocality in critical hybrid circuits, *Phys. Rev. B* **104**, 104305 (2021).
- [18] Y. Bao, S. Choi, and E. Altman, Theory of the phase transition in random unitary circuits with measurements, *Phys. Rev. B* **101**, 104301 (2020).
- [19] C.-M. Jian, Y.-Z. You, R. Vasseur, and A. W. W. Ludwig, Measurement-induced criticality in random quantum circuits, *Phys. Rev. B* **101**, 104302 (2020).
- [20] R. Fan, S. Vijay, A. Vishwanath, and Y.-Z. You, Self-organized error correction in random unitary circuits with measurement, *Phys. Rev. B* **103**, 174309 (2021).
- [21] Y. Bao, S. Choi, and E. Altman, Symmetry enriched phases of quantum circuits, *Ann. Phys.* **435**, 168618 (2021), special issue on Philip W. Anderson.
- [22] A. Bera and S. Singha Roy, Growth of genuine multipartite entanglement in random unitary circuits, *Phys. Rev. A* **102**, 062431 (2020).
- [23] S. Sang and T. H. Hsieh, Measurement-protected quantum phases, *Phys. Rev. Research* **3**, 023200 (2021).
- [24] L. Zhang, J. A. Reyes, S. Kourtis, C. Chamon, E. R. Mucciolo, and A. E. Ruckenstein, Nonuniversal entanglement level statistics in projection-driven quantum circuits, *Phys. Rev. B* **101**, 235104 (2020).
- [25] S. Choi, Y. Bao, X.-L. Qi, and E. Altman, Quantum error correction in scrambling dynamics and measurement-induced phase transition, *Phys. Rev. Lett.* **125**, 030505 (2020).
- [26] A. Nahum, S. Roy, B. Skinner, and J. Ruhman, Measurement and entanglement phase transitions in all-to-all quantum circuits, on quantum trees, and in Landau-Ginsburg theory, *PRX Quantum* **2**, 010352 (2021).
- [27] D. Rossini and E. Vicari, Measurement-induced dynamics of many-body systems at quantum criticality, *Phys. Rev. B* **102**, 035119 (2020).
- [28] J. Iaconis, A. Lucas, and X. Chen, Measurement-induced phase transitions in quantum automaton circuits, *Phys.*

- Rev. B **102**, 224311 (2020).
- [29] T. Kalsi, A. Romito, and H. Schomerus, Three-fold way of entanglement dynamics in monitored quantum circuits (2022), arXiv:2201.12259.
- [30] M. Szyniszewski, A. Romito, and H. Schomerus, Entanglement transition from variable-strength weak measurements, Phys. Rev. B **100**, 064204 (2019).
- [31] M. Szyniszewski, A. Romito, and H. Schomerus, Universality of entanglement transitions from stroboscopic to continuous measurements, Phys. Rev. Lett. **125**, 210602 (2020).
- [32] F. Haake, S. Gnutzmann, and M. Kuś, *Quantum Signatures of Chaos* (Springer, Berlin, 2018).
- [33] F. Haake, M. Kuś, and R. Scharf, Classical and quantum chaos for a kicked top, Z. Phys. B **65**, 381 (1987).
- [34] F. J. Dyson, A Brownian-motion model for the eigenvalues of a random matrix, J. Math. Phys. **3**, 1191 (1962).